
Quantitative microfluidic fluorescence microscopy to study vaso-occlusion in sickle cell disease

Maritza A. Jimenez,^{1,3} Egemen Tutuncuoglu,¹ Suchitra Barge,¹ Enrico M. Novelli,^{1,4} and Prithu Sundd^{1,2,3}

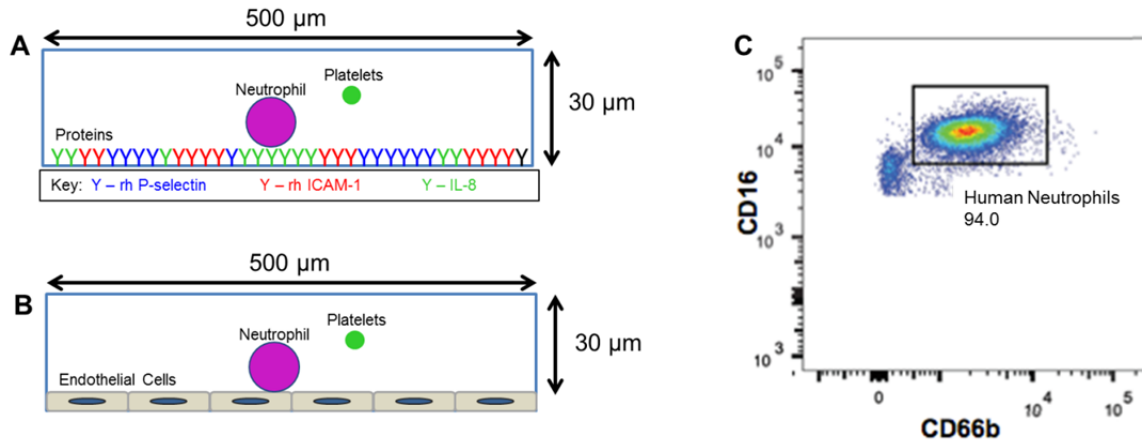
¹Heart, Lung, Blood and Vascular Medicine Institute; ²Division of Pulmonary, Allergy and Critical Care Medicine; ³Department of Bioengineering; and ⁴Division of Hematology and Oncology, University of Pittsburgh, Pittsburgh, PA, USA

*Correspondence: prs51@pitt.edu
doi:10.3324/haematol.2015.126631*

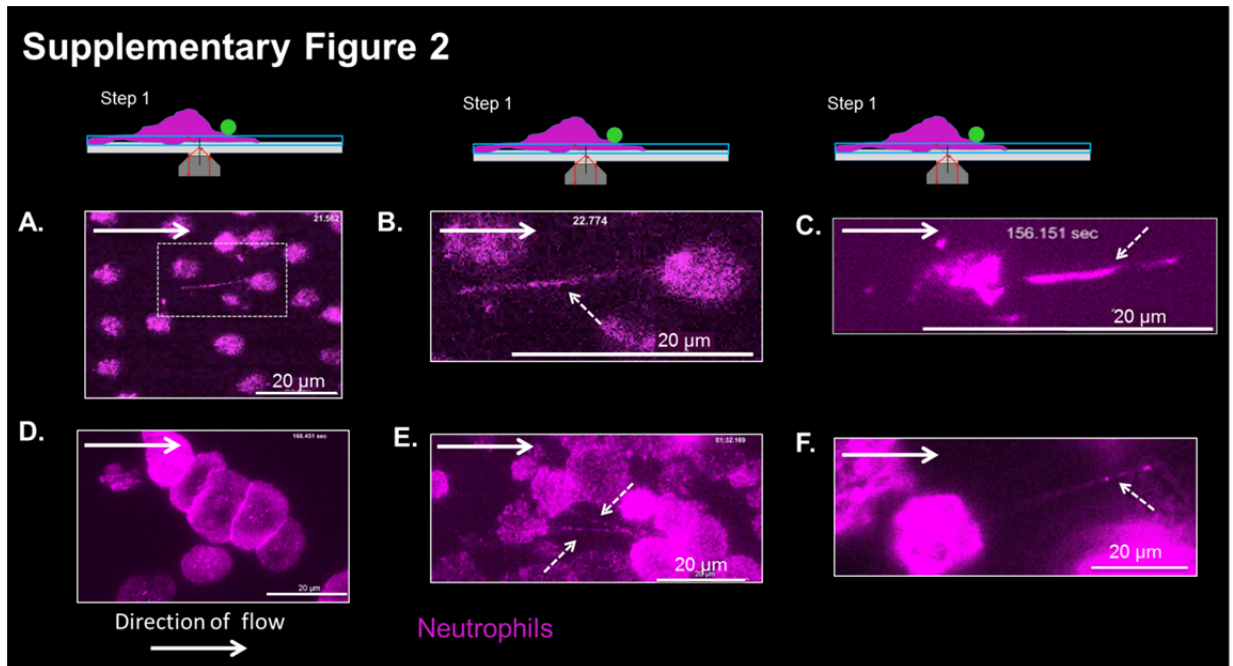
SUPPLEMENTARY INFORMATION

Table of contents

1. Supplementary Figures.
2. Legends for Supplementary Movies.
3. Materials and Methods.
4. References for Materials and Methods.

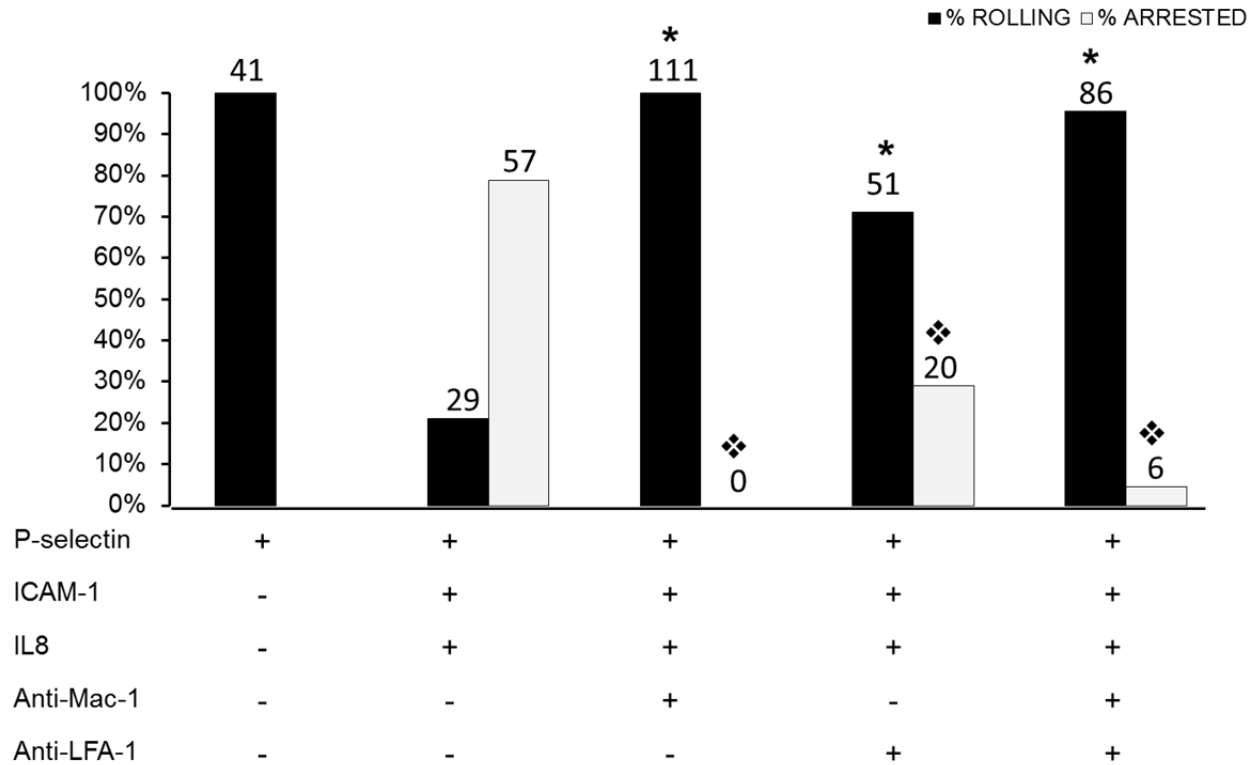


Supplementary Figure 1. (A-B) Cross-section of a micro-channel coated with (A) cocktail of P-selectin, ICAM-1 and IL-8 and (B) cultured endothelial cells along the grey dashed line shown in Figure 1A. (C) 94% of CD16⁺ cells in human blood are neutrophils (CD16⁺/CD66b⁺). Neutrophil (violet) and platelet (green) in A-B.



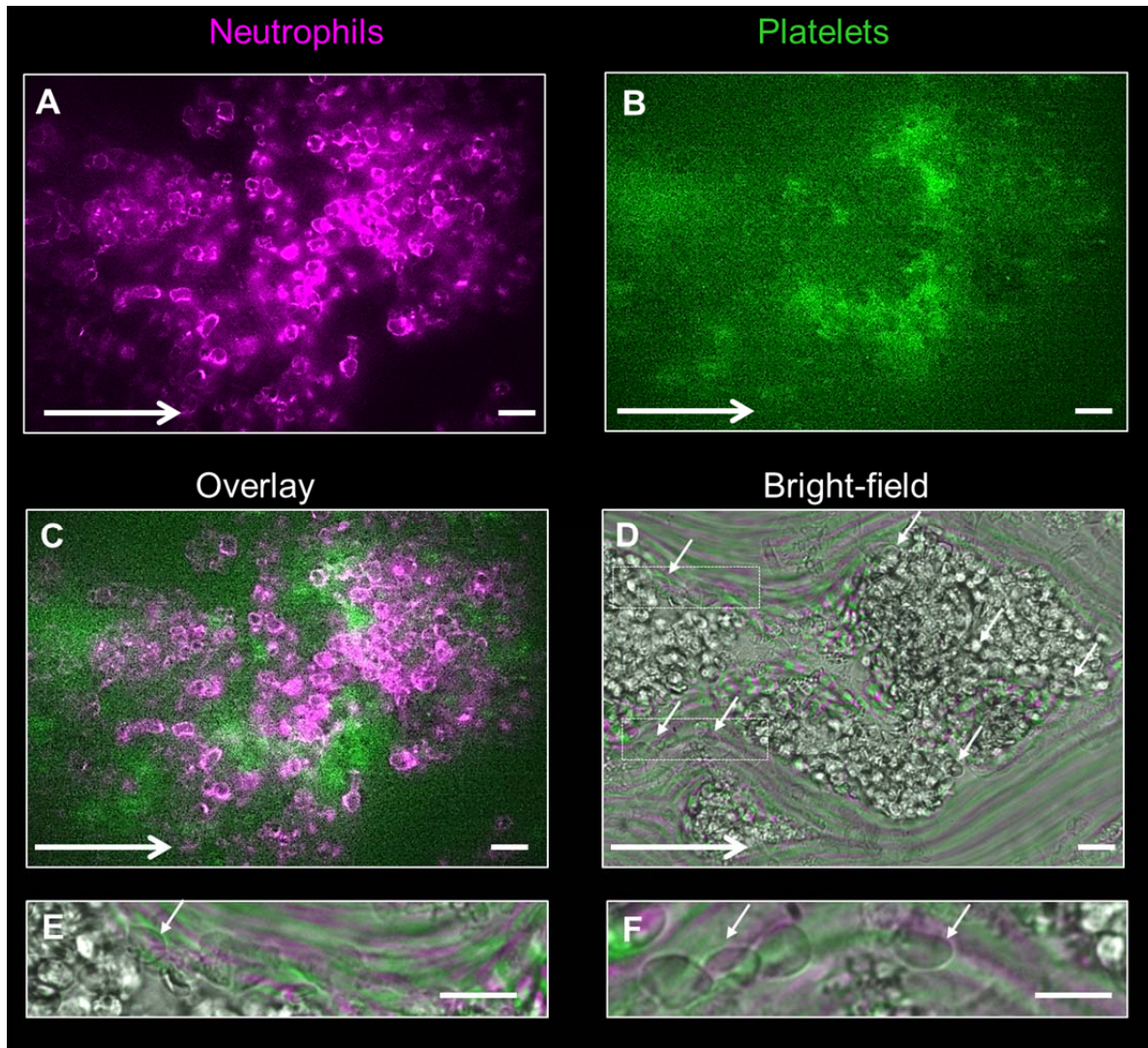
Supplementary Figure 2. qMFM reproduces rolling, arrest and sling formation by neutrophils in SS blood. SS or control human blood was perfused through microfluidic channels (shown in Supplementary Figure 1A) coated with P-selectin or a cocktail of P-selectin, ICAM-1 and IL-8. Footprints were recorded using imaging step-1. **(A)** Neutrophils rolling on P-selectin coated substrate in SS patient blood. Also refer Supplementary Movie 1. **(B)** Magnified view of the region marked with dotted box in A. A membrane tether (marked with dashed arrow) can be seen behind a rolling neutrophil. **(C)** Sling (marked with dashed arrow) in the front of a neutrophil rolling on a P-selectin coated substrate in control blood. Also refer Supplementary Movie 2. **(D)** Neutrophils arrest on P-selectin, ICAM-1, and IL-8 coated substrate in SS patient blood. Refer Supplementary Movie 3. **(E)** Slings (dashed arrows) can be observed to connect adjacent arrested neutrophils in SS patient blood. **(F)** Sling (marked with dashed arrow) exists on an arrested neutrophil in control human blood. Also refer Supplementary Movie 4. The schematic on top of each panel denotes the imaging strategy (step-1) used for visualization.

Horizontal arrows denote direction of blood flow. Wall shear stress 6 dyn cm^{-2} . Scale bars $20 \mu\text{m}$. Neutrophils (violet; AF647-anti-CD16 Ab). Excitation laser- 640 nm .



Supplementary Figure 3. Verification of adhesion specificity. Percent rolling and arrested neutrophils when control human blood was flown through P-selectin or P-selectin + ICAM-1 + IL-8 coated micro-channels either in presence or absence of function blocking Abs against Mac-1, LFA-1, P-selectin and PSGL-1. Numbers on top of bars represent total number of neutrophils. Fourfold table analysis with Bonferroni χ^2 -statistics was used to compare percentages between different groups. * $p < 0.01$ for rolling when compared with P-selectin, ICAM-1, IL-8 substrate without Ab treatment. ❖ $p < 0.01$ for arrest when compared with P-selectin, ICAM-1, IL-8 substrate without Ab treatment. Blocking of P-selectin on substrate or PSGL-1 on neutrophils completely abolished neutrophil rolling and arrest (data not shown). Data representative of two experiments with at least two FOVs per experiment. Percents were estimated by dividing total number of rolling or arresting neutrophils in all the FOVs by the total number of neutrophils

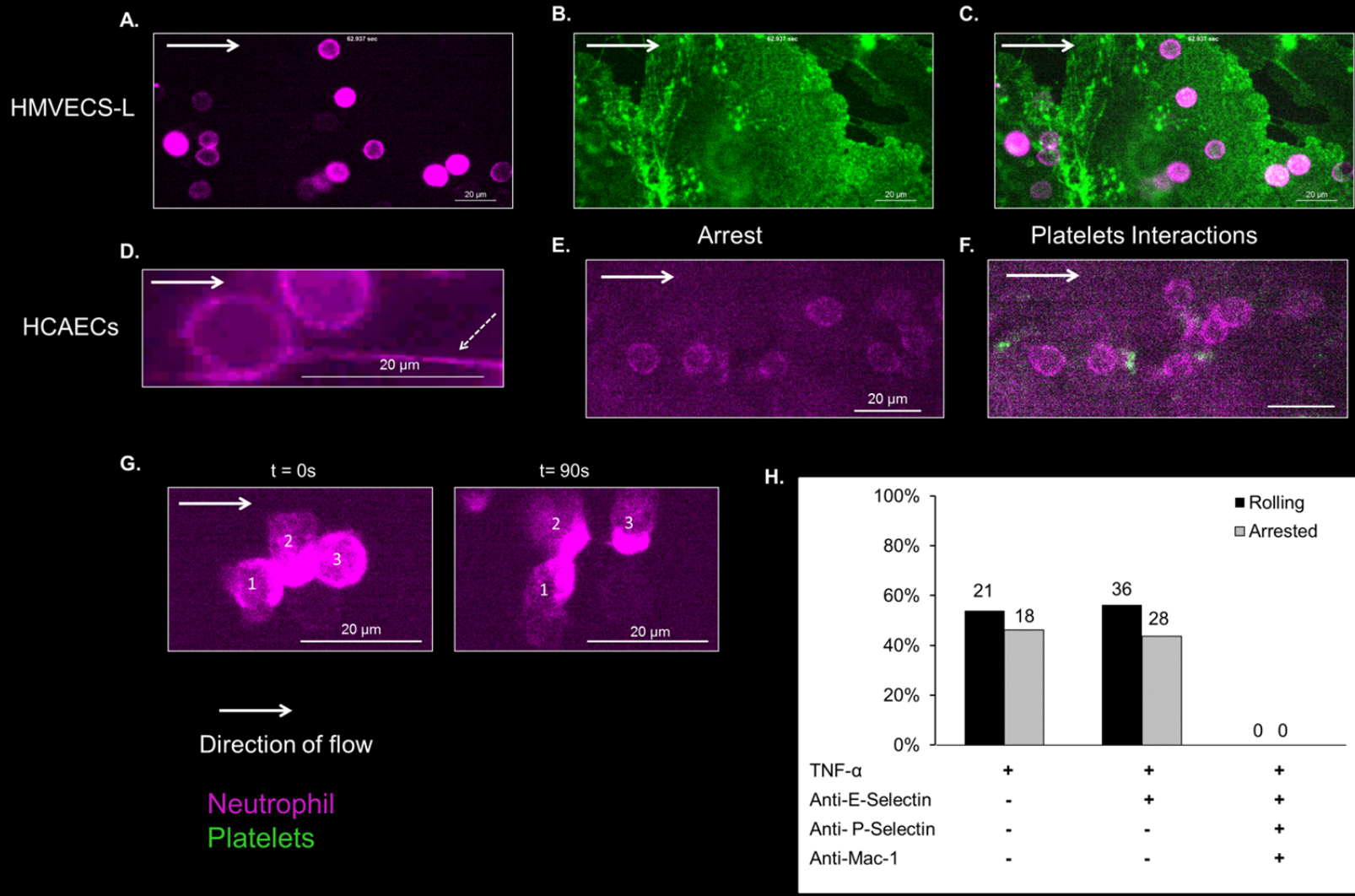
(rolling and arrested) in all the FOVs for each condition. Wall shear stress = 6 dyn cm^{-2} , FOV \sim $14,520 \text{ } \mu\text{m}^2$.



Supplementary Figure 4. Occlusion of microfluidic channel with platelet-neutrophil-RBC aggregates. SS blood was perfused through microfluidic channels (shown in Supplementary Figure 1A) coated with a cocktail of P-selectin, ICAM-1 and IL-8. **(A)** The violet channel image showing partial occlusion of the microfluidic channel by arrested neutrophils (violet). **(B)** Green channel image showing presence of platelet aggregates (green) in the same FOV shown in A. **(C)** Overlay of violet and green channels demonstrates that the microfluidic channel shown in A and B is partially occluded by the aggregation of platelets (green) on top of arrested neutrophils (violet). **(D)** Bright field image of the same FOV shown in A-C reveals RBCs trapped in the

platelet-neutrophil aggregate occluding the microfluidic channel. Representative RBCs have been marked with small white arrows in D. **(E-F)** Regions marked with dashed boxes in D magnified to reveal RBCs (marked with white arrows) trapped in the platelet-neutrophil aggregate. Horizontal arrows denote blood flow direction. Scale bars 20 μm . Neutrophil (violet; AF647-anti-CD16 Ab), platelet (green; FITC-anti-CD49b Ab). Fluorescent images in A-C visualized using imaging step-2. Image in D visualized with bright-field microscopy. Excitation lasers-488 nm and 640 nm.

Supplementary Figure 5



Supplementary Figure 5. Neutrophil adhesion and platelet-neutrophil interactions on cultured endothelium. SS or control human blood was perfused through microfluidic channels cultured with TNF- α activated HMVECs-L or HCAECs. Adhesive events were visualized using imaging step-2. **(A-C)** Neutrophils (violet) rolling or arresting on TNF- α activated HMVECs-L in control human blood. HMVECs-L were stained with PE-anti-PECAM-1 mAb (pseudo-colored green) visible as green staining along the cell borders. Also refer Supplementary Movie 6. **(A)** The violet channel showing rolling or arresting neutrophils. **(B)** The green channel showing the HMVECs-L. **(C)** Overlay of A and B showing neutrophils (violet) rolling or arresting on HMVECs-L (green). **(D)** Sling (marked with dashed arrow) formation by neutrophil rolling on HCAECs in control human blood. **(E)** Neutrophil arrest on TNF- α activated HCAECs in SS patient blood. **(F)** Platelets (green) interacting with neutrophils (violet) that are arrested on TNF- α activated HCAECs in SS patient blood. **(G)** Neutrophils crawling on TNF- α activated HCAECs in control human blood. Three neutrophils interacting with each other at 0 s start to migrate away by 90 s. Numbers identify individual neutrophils over time. **(H)** Neutrophil rolling and arrest in SS patient blood was not effected by blocking E-selectin on HCAECs but completely abolished by blocking Mac-1 (CD11b/CD18) on neutrophils and P-selectin on HCAECs. Numbers on top of bars denote total number of neutrophils. Representative of three experiments and five FOVs. Percents were estimated by dividing total number of rolling or arresting neutrophils in all the FOVs by the total number of neutrophils (rolling and arrested) in all the FOVs for each condition. Fourfold table analysis with Bonferroni χ^2 -statistics was used to compare percentages between different groups. Neutrophil (violet; AF647-anti-CD16 Ab), platelet (green; FITC-anti-CD49b Ab). Horizontal arrows denote blood flow direction. Wall shear stress = 6 dyn cm⁻². Scale bars 20 μ m. Excitation lasers-488 nm, 561 nm and 640 nm.

LEGENDS FOR SUPPLEMENTARY MOVIES

Supplementary Movie 1. Neutrophils rolling on P-selectin coated substrate in SS patient blood. Wall shear stress 6 dyn cm^{-2} . Neutrophils (violet; AF647-anti-CD16 Ab). Excitation laser- 640 nm. Imaging step-1. 30x of original frame rate.

Supplementary Movie 2. Sling formed by a neutrophil rolling on a P-selectin coated substrate in control human blood. Wall shear stress 6 dyn cm^{-2} . Neutrophils (violet; AF647-anti-CD16 Ab). Excitation laser- 640 nm. Imaging step-1. 8x of original frame rate.

Supplementary Movie 3. Transition from rolling to arrest on P-selectin, ICAM-1, and IL-8 coated substrate in SS patient blood. Wall shear stress 6 dyn cm^{-2} . Neutrophils (violet; AF647-anti-CD16 Ab). Excitation laser- 640 nm. Imaging step-1. 50x of original frame rate.

Supplementary Movie 4. Sling present on a neutrophil arrested on P-selectin, ICAM-1, and IL-8 coated substrate in control human blood. Wall shear stress 6 dyn cm^{-2} . Neutrophils (violet; AF647-anti-CD16 Ab). Excitation laser- 640 nm. 10x of original frame rate.

Supplementary Movie 5. Sequential use of imaging step-1 and 2 to visualize footprints of crawling neutrophils and platelets nucleating on crawling neutrophils, respectively. P-selectin, ICAM-1, and IL-8 coated substrate. Control human blood. Wall shear stress 6 dyn cm^{-2} . Neutrophils (violet; AF647-anti-CD16 Ab). Platelet (green; FITC-anti-CD49b Ab). Excitation laser- 640 and 488 nm. 10x of original frame rate.

Supplementary Movie 6. Neutrophils rolling and arresting on TNF- α activated HMVECs-L in control human blood. HMVECs-L (green; PE-anti-PECAM-1 Ab). Neutrophils (violet; AF647-anti-CD16 Ab). Wall shear stress 6 dyn cm⁻². Excitation laser- 640 and 561 nm. 10x of original frame rate. Imaging step-2.

Supplementary Movie 7. Neutrophils crawling on TNF- α activated HCAECs in control human blood. Wall shear stress 6 dyn cm⁻². Neutrophils (violet; AF647-anti-CD16 Ab). Excitation laser- 640 nm. 30x of original frame rate. Imaging step-2.

MATERIALS AND METHODS

Reagents

Recombinant human P-selectin-Fc chimera (P-selectin) and recombinant human ICAM-1-Fc chimera (ICAM-1) were purchased from R&D Systems (Minneapolis, MN). Recombinant human CXCL8/interleukin-8 (IL-8) was purchased from Peprotech Inc. (Rocky Hill, NJ). Alexa Fluor-647 conjugated mouse anti-human CD16 mAb (clone 3G8, mouse IgG1), FITC conjugated mouse anti-human CD49b mAb (clone AK-7, mouse IgG1), FITC conjugated mouse anti-human CD66b (clone G10F5, mouse IgG1), function blocking purified NA/LE mouse anti-human CD11b mAb (clone ICFR44, mouse IgG1), mouse anti-human CD162 (clone KPL-1, mouse IgG1), PE-conjugated anti-human PECAM-1 (clone WM59, mouse IgG1) and isotype control mouse IgG1 were purchased from BD Biosciences (San Jose, CA). Function blocking anti-human CD62P mAb (clone G1/G14, mouse IgG1), anti-human CD62E mAb (clone HAE-1f, mouse IgG1) were purchased from Ansell Corp. (Bayport, MN). Function blocking anti-human CD11a mAb (clone TS1/22, mouse IgG1) was purchased from Thermo Scientific™ (Rockford, IL). Human fibronectin was purchased from Fisher Scientific, (Pittsburgh, PA). Recombinant human tumor necrosis factor- α (TNF- α) was purchased from Peprotech, Inc.

Blood collection

Blood samples were collected from 8 race-matched control and 10 SS patients in accordance with the guidelines set by the Institutional Review Board at the University of Pittsburgh. Informed written consent was obtained from all the participants in accordance with the Declaration of Helsinki. Non-smokers who were not on chronic blood transfusion or hydroxyurea therapy or were non-compliant to hydroxyurea were included in the study. Blood

was drawn via venipuncture using a 21G needle (BD Biosciences) into a 10 ml syringe filled with 20 U/ml of heparin (Henry Schein, Melville, NY) or 25 U/ml hirudin (Sigma Aldrich, St. Louis, MO). Fluorescent antibodies against human CD16 (3 μ l) and CD49b (2.5 μ l) were added to 500 μ l of blood in a 1 ml eppendorf tube to stain neutrophils and platelets *in situ*, respectively. Also, complete blood cell counts were conducted using Hemavet® HV950 (Drew Scientific, Miami Lakes, FL). All experiments were completed within 2 hours of blood draw and the blood sample was gently mixed on a rocker mixer during the entire experiment.

Flow cytometry

Heparinized blood was lysed with 1X RBC lysis buffer (eBioscience, San Diego, CA) and cells were suspended in PBS without Ca^{2+} and Mg^{2+} + 1% BSA + 0.1% sodium azide, pH 7.4. The cell suspension was incubated with FITC-CD66b (1:100) and AlexaFluor647-CD16 (1:100) mAbs or isotype matched control Abs and analyzed on BD-Fortessa flow cytometer (BD). Post-acquisition analysis was done using FlowJo software.

Endothelial cell culture and activation

Clonetics™ human coronary artery endothelial cells (HCAECs) or human lung micro-vascular endothelial cells (HMVECs-L) were grown in endothelial cell basal medium-2 (EBM-2; Lonza, Walkersville, MD) at 37°C and 5% CO_2 in a CO_2 incubator. The medium was supplemented with endothelial cell growth medium kit (EGM-2 MV SingleQuots; Lonza) which consists of 10% FBS, hydrocortisone, hFGF-B, VEGF, R3-IGF-1, ascorbic acid, hEGF and GA-1000. Cells used for the experiments were not higher than the 12th passage and reached confluence in 5 days.

Preparation of adhesion molecule presenting substrates

The coating of cover slips with recombinant adhesion molecules has been described in detail elsewhere¹. Rectangular coverslips (No. 1.5, Fisher Scientific) were coated with a cocktail of 2 µg/ml of P-selectin, 10 µg/ml of ICAM-1 and 10 µg/ml of IL-8 followed by incubation at room temperature for 30 min. P-selectin coating concentration of 2 µg/ml has been shown previously to result in a molecular density of ~20 molecules/µm², which is comparable to the P-selectin molecular density on cultured endothelial cells^{1,2}. Following the incubation, the coverslips were washed once with phosphate buffered saline without Ca²⁺ and Mg²⁺ (PBS; MP Biomedicals, Solon, OH) and incubated in 2 ml of blocker casein (Thermo Scientific™, Rockford, IL) until used in assay to block all nonspecific binding sites.

Preparation of endothelialized substrates

A 12 mm² region on rectangular cover slips (Number 1.5, Fisher Scientific) was coated with 10 µg/ml of human fibronectin for 30 minutes at room temperature and 20,000 HMVECs-L or HCAECs in 50 µl culture medium (400,000 cells/ml) were allowed to adhere to the coated region. Cells were allowed to reach confluence at 37°C and 5% CO₂ in a CO₂ incubator for 5 days. Once confluent, cells were activated by overnight incubation with 100 ng/ml recombinant human TNF-α and used in microfluidic flow assays.

Microfluidic flow assay

Assembly of microfluidic devices has been described elsewhere in detail^{1,3,4}. A PDMS/silicone chip with micro-channels engraved on its surface was gently placed on a glass coverslip (Figure 1A) either coated with a cocktail of P-selectin, ICAM-1, and IL-8 (Supplementary Figure 1A) or

cultured with TNF- α treated HMVECs-L or HCAECs (Supplementary Figure 1B) and sealed together using vacuum (negative 30 KPa pressure). Prior to blood perfusion, the endothelialized microfluidic devices were filled with a KREBS-HEPES buffer, pH 7.4 (NaCl, KCl, MgSO₄, NaHCO₃, KH₂PO₄, HEPES, Glucose and CaCl₂) to keep the endothelial monolayer viable. The assembled device had an inlet, an outlet, a vacuum port connected to in-house vacuum supply and four identical micro-channels or perfusion chambers (30 μ m high and 500 μ m wide) with nearly identical flow rates and wall shear stresses. The wall shear stress was calibrated as a function of the differential pressure between the inlet and outlet reservoir. The differential pressure was set by placing the inlet reservoir next to the device while lowering the outlet reservoir to achieve the physiological wall shear stress⁵ of 6 to 10 dyn cm⁻². Approximately 500 μ L of anti-coagulated blood was transferred to a 1.5 mL eppendorf tube which served as an inlet reservoir while a 10 ml syringe filled with PBS served as the outlet reservoir. The inlet and outlet reservoirs were connected to the inlet and outlet ports of the device using PE10 (ID 0.28 mm, OD 0.61 mm; BD, Sparks, MD) and TYGON (ID 0.8 mm, OD 2.4 mm; Fisher Scientific) tubing, respectively. CD49b is the α 2 chain of the collagen receptor α 2 β 1 on platelets and has been used previously to identify platelets in blood⁶. CD16 has been used previously⁷ to identify human neutrophils which are defined as double positive for CD66b⁺ and CD16⁺. Our flow cytometry data (Supplementary Figure 1C) revealed that 94% of CD16⁺ cells in human blood are neutrophils as they are also CD66b⁺. Based on this Alexa Fluor 647 conjugated anti-human CD16 and FITC-conjugated anti-human CD49b Abs to stain neutrophils and platelets, respectively, were added to the blood (3:500 CD16; 1:250 CD49b) in the inlet reservoir. Adhesion specificity was confirmed by either incubating the adhesion molecule or endothelial cells coated cover slips with function blocking Abs against P-selectin (1:500) and E-selectin

(1:500) for 10 min at 37°C/5% CO₂ prior to their use in microfluidic assay. In some experiments, function blocking Abs against Mac-1, LFA-1 and PSGL-1 were added to the blood (1:100) in the inlet reservoir followed by 10 min of incubation with mixing at room temperature prior to use in the microfluidic assay. Finally, the microfluidic device was placed on the heated stage set at 24° or 37°C (Okolab, Ottaviano, Italy) of an inverted microscope and the blood was perfused through the micro-channels at a wall shear stress of 6 to 10 dyn cm⁻². Observations were made in the perfusion chambers (Supplementary Figure 1A and B; 30 μm high and 500 μm wide).

Estimation of wall shear stress in qMFM

The differential pressure across the inlet and outlet of the microfluidic device was set by placing the inlet reservoir on the microscope stage (next to the device) while lowering the outlet reservoir relative to the inlet reservoir to achieve a difference in height 'Δh' (Figure 1A). A 1% suspension of yellow-green 1 μm Fluoresbrite® microspheres (Polysciences Inc, Warrington, PA) in PBS was allowed to flow through the microfluidic device and the center-line velocity of the beads in the micro-channels was estimated by measuring the maximum bead velocity (v_{max}) at H/2 (H = 30 μm is the height of the micro-channel in Supplementary Figure 1A-B) using fluorescence microscopy. Wall shear stress (τ in dyn cm⁻²) at a chosen differential pressure (Δh) was estimated as $4\eta v_{max}/H$, where η is the viscosity of plasma (1 centipoise)⁸. All the observations were made at a physiological wall shear stress⁵ of 6 dyn cm⁻² which was achieved with a Δh of 10.6 inches.

Quantitative Dynamic Footprinting (qDF)

qDF is an adaptation of total internal reflection fluorescence (TIRF) microscopy that allows

visualization of the footprints of rolling and arresting neutrophils on a glass substrate coated with endothelial adhesion molecules¹. A laser is incident through a high numerical aperture, high magnification, oil immersion objective at the glass-cell interface at an angle (70°) greater than the critical angle, θ_c (64.33°) = $\sin^{-1}(n_2/n_1)$, where $n_1 = 1.52$ and $n_2 = 1.37$ ($n_1 > n_2$) are the refractive index of glass and cell cytoplasm, respectively. The laser is completely reflected back into the objective but an evanescent wave (light blue box in Figure 1B) is established on the cell side of the cover slip. The intensity of the evanescent wave decreases with z-distance and becomes negligible within 200 nm above the cover slip (light blue box in Figure 1B). As a result, fluorescence is excited only in the cell membrane and cytosolic region that lies within 200 nm above the cover slip, while the remainder of the cell remains invisible.

Strategy for analyzing qMFM data

The following strategy was followed in Figures 2, 3 and Supplementary Figures 2-4 to record observations in adhesion molecule coated micro-channels.

Step-1: Neutrophils were allowed to roll, arrest and crawl for 2 min and observations were recorded in a field of view (FOV~ $14,520 \mu\text{m}^2$) using qDF (shown in Figure 1B).

Step-2: After 2 min, the incident angle of the laser was reduced (shown in Figure 1C) and the platelet-neutrophil interactions were observed in the same FOV for an additional 4 min.

As the thickness of endothelial monolayer is greater than 200 nm, only step-2 (epi-fluorescence) was used to record observations in endothelialized micro-channels in Supplementary Figure 5.

Time series sequences of images were processed and analyzed using NIS-Elements Analysis Advanced Research software (Nikon). Image background was subtracted using the average intensity of a small region of the image background and platelets were identified using the spot-

detection algorithm available in NIS-Elements. The interacting platelets are marked with white circles in Figure 3D. The spot-detection algorithm identifies only those platelets which slowdown to interact with arrested neutrophils and continues to track them until they detach and leave the FOV. Platelets are identified by defining a threshold based on the intensity and size of the bright spots. The final read-out is the number of interactions in a given observation period and the life-time of each interaction. Platelet-Neutrophil interactions were defined as following:

- A freely flowing platelet attaches to an arrested neutrophil → an interaction event.
- A freely flowing platelet aggregate attaches to an arrested neutrophil → an interaction event.
- A rolling neutrophil enters the FOV with a platelet attached to it → an interaction event.
- A platelet or an aggregate of platelets detaches from one neutrophil and attaches to another neutrophil → an interaction event.

Mean of total events under different conditions were compared using student's *t*-test (Figure 3E). Lifetimes of interactions under different conditions were compared as cumulative probability distributions (Figure 3F) using non-parametric Kruskal-Wallis *H*-test.

Microscope set-up

Experiments were conducted using a Nikon Eclipse-Ti inverted microscope with a TIRF photo-activation unit (NIKON, Melville, NY). The microscope was equipped with a Zyla-5.5 sCMOS scientific camera (5.5 Megapixel resolution; maximum frame rate 100 s⁻¹; ANDOR, South Windsor, CT) and a motorized Nikon Intensilight CHGFIE fiber illuminator as an epifluorescence source. Lasers were housed in a MLC Monolithic Laser combiner launch (Agilent Technologies, Santa Clara, CA) and included 405 nm, 488 nm, 560 nm, and 640 nm

wavelength lasers. Observations were made using a CFI Apochromat TIRF 60x oil objective (NA 1.49) or CFI Plan Fluor ELWD 40x air objective (NA 0.60). The laser, camera, filters and other microscope functions were controlled using NIS-Elements software (Nikon) installed on a PC. NIS-Elements allowed sequential capture of green (FITC) and far red channel (Alexa Fluor 647) through a quad-filter by switching between the two lasers at a minimum interval of 10 ms which generated a dual color image every 20 ms.

Scanning Electron Microscopy

Freshly collected whole blood was perfused over a rectangular coverslip coated with P-selectin, ICAM-1 and IL-8 in a custom PDMS vacuum chip (shown in Figure 1A) at a wall shear stress of 6 dyn cm^{-2} . Neutrophils were allowed to roll and arrest on the coverslip and interact with freely flowing platelets. Following a 3-minute perfusion, a cocktail of 16% paraformaldehyde and 2.5% glutaraldehyde was perfused through the micro-channels at the same shear stress (6 dyn cm^{-2}) to fix platelet-neutrophil interactions under flow. Finally, the vacuum was disabled and the coverslips were separated from the PDMS chip. Fixed coverslips were stored in the fixative cocktail until used in electron microscopy. Processing of coverslips for electron microscopy has been described elsewhere in detail⁹. Coverslips were cut, sputter coated with gold and visualized using a Field Emission Scanning Electron Microscope (JEOL JSM 6335F).

Statistical Analysis

Mean number of platelet-neutrophil interactions under different conditions were compared using a student's *t*-test (Figure 3E). Non-parametric Kruskal-Wallis *H*-test was used to analyze the difference in the platelet-neutrophil interaction time distributions between different groups in

Figure 3F. Fourfold table analyses with Bonferroni χ^2 -statistics were used to compare percentages between different groups (Supplementary Figure 3 and Supplementary Figure 5H). A p -value of less than 0.05 was used to determine significance.

Advantages and Limitations of qMFM

There are several advantages in using qMFM to study vaso-occlusion. Collection of large volumes of blood from SS patients can be challenging as these patients suffer from chronic anemia¹⁰. The volumetric flow rate through microfluidic device used in qMFM (Figure 1A) is 12 $\mu\text{l min}^{-1}$ at a wall shear stress of 6 dyn cm^{-2} . Thus qMFM allows 4 min long experimental observations using as little as 50-100 μl of anti-coagulated blood. Also the microfluidic chips are reusable, easy to fabricate and cost less than 10 cents per chip¹. On top of that a two-step fluorescence microscopy approach (Figure 1B-C) provides a choice of studying either footprints of crawling neutrophils or neutrophil-platelet aggregation with a swift transition between the steps. This strategy of visualizing neutrophil footprints without platelets and RBCs in the background can be useful in determining the effect of anti-adhesion drugs on neutrophil rolling and arrest vs. neutrophil-platelet aggregation. Neutrophils and platelets were the only blood cells visualized in the current study; however, the *in situ* fluorescence staining can be easily extended to visualize RBCs and other leukocytes like monocytes, iNKT-cells and NK cells which are known to play a role in VOC¹¹⁻¹³. In addition to SEM (shown in Figure 3G), the interacting cells fixed under flow and stained with fluorescent Abs against adhesion molecules or cytoskeletal proteins can be visualized using super-resolution fluorescence microscopic techniques like Structured-Illumination-Microscopy (SIM) or STimulated Emission Depletion (STED) microscopy which are capable of visualizing cellular features at an unprecedented lateral

resolution of 100 nm and 20 nm, respectively. qMFM can also serve to understand the pathophysiology of vaso-occlusion driven by diverse inflammatory stimuli like bacterial lipopolysaccharides (LPS), hemin or adenosine-di-phosphate (ADP). SS blood can be incubated with LPS or ADP or hemin and the effect on platelet-neutrophil interaction can be assessed by using qMFM to measure the interaction time and total interactions both in presence or absence of anti-adhesion or anti-inflammatory drugs. qMFM can also be used to visualize reactive oxygen species (ROS) production by specific cell types in SS blood under flow. Blood can be incubated with MitoSox-Red or Dihydroethidium (both commercially available from Life Technologies) to visualize superoxide generation within the mitochondria or cytosol, respectively, of cells interacting under flow. Although qMFM is a useful tool, there are few limitations associated with this approach. The blood has a tendency to coagulate on coming in contact with silicone or glass. To avoid artifacts, microscopic observations in a single microfluidic chip should be limited to not more than six minutes. However, the low cost of microfluidic chips and their ability to be recycled circumvents this limitation. Anti-coagulated blood tends to coagulate and separate into plasma and cell pellet when allowed to sit without any mixing. Our pilot studies (data not shown) revealed that in order to eliminate artifacts, the anti-coagulated blood needs to be mixed continuously and used in qMFM within 2 hours following blood collection thus allowing less time for data collection. qMFM requires *in situ* staining of blood cells by addition of fluorescent Abs against lineage markers to blood. In order to visualize different blood cell types distinctly, it requires selection of fluorochromes with distinct excitation and emission spectra for each blood cell type so that cell types can be identified based on the emission spectra. However, with the advent of commercially available multi-wavelength laser and LED sources as well as high-

sensitivity sCMOS cameras, video-rate sequential acquisition of at least four fluorochromes is easily achievable.

References

1. Sundd P, Gutierrez E, Pospieszalska MK, Zhang H, Groisman A, Ley K. Quantitative dynamic footprinting microscopy reveals mechanisms of neutrophil rolling. *Nature Methods*. 2010;7(10):821-824.
2. Hattori R, Hamilton K, Fugate R, McEver R, Sims P. Stimulated secretion of endothelial von Willebrand factor is accompanied by rapid redistribution to the cell surface of the intracellular granule membrane protein GMP-140. *J Biol Chem*. 1989;264(14):7768-7771.
3. Sundd P, Gutierrez E, Petrich BG, Ginsberg MH, Groisman A, Ley K. Live cell imaging of paxillin in rolling neutrophils by dual-color quantitative dynamic footprinting. *Microcirculation*. 2011;18(5):361-372.
4. Tkachenko E, Gutierrez E, Ginsberg MH, Groisman A. An easy to assemble microfluidic perfusion device with a magnetic clamp. *Lab Chip*. 2009;9(8):1085-1095.
5. Damiano ER, Westheider J, Tozeren A, Ley K. Variation in the velocity, deformation, and adhesion energy density of leukocytes rolling within venules. *Circ Res*. 1996;79(6):1122-1130.
6. Jenne CN, Wong CH, Petri B, Kubes P. The use of spinning-disk confocal microscopy for the intravital analysis of platelet dynamics in response to systemic and local inflammation. *PLoS One*. 2011;6(9):e25109.
7. Yipp BG, Petri B, Salina D, et al. Infection-induced NETosis is a dynamic process involving neutrophil multitasking in vivo. *Nat Med*. 2012;18(9):1386-1393.
8. Bird RB, Stewart WE, Lightfoot EN. *Transport Phenomena*. First ed. New York: John Wiley & Sons, Inc., 1960.

9. Sundd P, Gutierrez E, Koltsova EK, et al. 'Slings' enable neutrophil rolling at high shear. *Nature*. 2012;488(7411):399-403.
10. Rees DC, Williams TN, Gladwin MT. Sickle-cell disease. *Lancet*. 2010;376(9757):2018-2031.
11. Wallace KL, Linden J. Adenosine A2A receptors induced on iNKT and NK cells reduce pulmonary inflammation and injury in mice with sickle cell disease. *Blood*. 2010;116(23):5010-5020.
12. Chantrathammachart P, Mackman N, Sparkenbaugh E, et al. Tissue factor promotes activation of coagulation and inflammation in a mouse model of sickle cell disease. *Blood*. 2012;120(3):636-646.
13. Zennadi R. MEK inhibitors, novel anti-adhesive molecules, reduce sickle red blood cell adhesion in vitro and in vivo, and vasoocclusion in vivo. *PLoS One*. 2014;9(10):e110306.